Decentralized SISO Active Disturbance Rejection Control of the Newell-Lee forced circulation evaporator

Rainer Dittmar

West Coast University of Applied Sciences, Heide, Germany
(Tel: +49 481 8555-325; e-mail: dittmar@fh-westkueste.de)

Abstract: Active Disturbance Rejection Control (ADRC) has received considerable attention in recent years as an effective tool for advanced control practitioners to solve control problems for nonlinear uncertain systems. This paper presents results of a simulation study for the control of an evaporator system benchmark, when a multiple linear ADRC control structure is used, and the controllers are designed based on first and second order linear models approximating the process dynamics. In addition to the control performance under nominal conditions, the robustness with respect to plant-model mismatch is studied. The major advantage of ADRC compared to MPC and PI control approaches is the simple and transparent tuning, and that only a coarse process model is sufficient for the design. For a broader industrial application of ADRC in the process industries, user-friendly off-line design tools as well as real-time ADRC control software for PLCs and DCS still have to be developed.

Keywords: Process control, Disturbance rejection, Decentralized control, PID control.

1. INTRODUCTION

It is not a new statement that more than 95% of the controllers applied in the process industries are variants of the single-loop PID controller (Ogunnaike and Mukati, 2006). In order to overcome its limitations, several alternatives have been developed including SISO-constrained LQ control (Pannocchia, Laachi and Rawlings, 2005), RTD-A control (Ogunnaike and Mukati, 2006), Predictive Functional Control (Richalet and O'Donovan, 2009) and SISO Model Predictive Control (Lu, 2004; Morrison, 2005). Only PFC and single-loop MPC have been implemented on DCS and PLCs yet, and the number of industrial applications is still small.

Recently, a new control paradigm named "Active Disturbance Rejection Control" (ADRC) has been introduced which also claims to be a potential candidate for PID replacement (Han, 2009) and a promising addition to the toolbox of control engineering practitioners (Rhinehart, Darby and Wade, 2011). ADRC is an unconventional design strategy. The key difference to other controllers is that ADRC uses a so-called extended state observer (ESO) which jointly estimates external disturbances and modelling uncertainties, and a control algorithm compensating the effect of this "generalized disturbance". In contrast to MPC, only loose process information is required. On the other hand, the tuning of the ESO as well as the control algorithm itself is simpler and more transparent as PID controller tuning. For more detailed information on the theoretical background and the properties of ADRC, the reader is referred to (Gao, 2006; Huang and Xue, 2014; Zheng and Gao, 2014).

An extensive list of industrial applications of ADRC is provided on the Center for Advanced Control Technologies website of the Cleveland State University (www.cact.csuohio.edu), some of them are briefly described in (Chen, Zheng and Gao, 2007). They include drive and motion control, robotics, power converters and superconducting RF cavities. To our knowledge, applications in the process industries are rare: they include web tension control and the control of a hose extrusion plant at Parker Hannifin Inc. Nevertheless, simulation studies have been published which demonstrate the application of ADRC to process control problems. In (Chen, Zheng and Gao, 2007), ADRC is applied to (a) temperature and (b) outlet concentration control of nonlinear continuous stirred tank reactor (CSTR) models. In (Zheng, Chen and Gao, 2009), a multivariable CSTR model is used to demonstrate multi-loop linear ADRC control, where the process dynamics is approximated with first order transfer functions. Huang and Xue (2013) apply multi-loop ADRC control to the ALSTOM gasifier benchmark problem. Again, first order process dynamics is assumed to design the observer/controller system for three pairs of manipulated and controlled variables. In all cases, simulations are carried out using only the nominal process model of the plant.

In this paper, ADRC is applied to the evaporator system benchmark originally developed by Newell and Lee (1989). The evaporator model is not too difficult but nevertheless convenient to demonstrate the application of advanced control technologies to a nonlinear multivariable system with strong interactions. Recently, this example has been used to design an offset-free 2x2 MPC controller based on ARX models identified from virtual plant tests (Huusom and Jorgensen, 2014). In the present paper, a decentralized multi-loop control structure with two linear ADRC controllers is designed. First and second order transfer function models are identified from virtual plant tests. They establish the basis for the design and tuning of the observers/control laws. In addition to setpoint tracking and (external and internal) disturbance rejection performance, the robustness in case of plant-model mismatch is studied.

The remainder of this paper is organized as follows. Section 2 gives an introduction into the design and tuning of linear SISO ADRC controllers. In Section 3, the evaporator system model is briefly described. Section 4 presents results of a simulation study for the multi-loop ADRC controlled evaporator system focussed on control performance and robustness. Finally, Section 5 presents conclusions and open problems.

2. ADRC DESIGN AND TUNING

In this section, following (Zheng and Gao, 2014) and (Herbst, 2013), the linear ADRC design is described for a second order process with steady state gain K, natural period T and damping factor D

$$T^2\ddot{y}(t) + 2DT\,\dot{y}(t) + y(t) = K\,u(t) \tag{1}$$

Adding an input disturbance $d(t)$, dividing by T^2, and abbreviating $a = K/T^2$ leads to

$$\begin{aligned}\ddot{y}(t) &= \underbrace{\left(-\frac{2D}{T}\dot{y}(t) - \frac{1}{T^2}y(t) + \frac{1}{T^2}d(t) + \Delta a\,u(t)\right)}_{generalized\ disturbance\ f(t)} + a_0 u(t)\\ &= f(t) + a_0 u(t)\end{aligned} \tag{2}$$

Here, a is splitted into a known part a_0 and an unknown modelling error Δa, i.e. $a = a_0 + \Delta a$. The total disturbance term $f(t)$ includes both internal uncertainties (unknown dynamics) and process parameter variations, and external disturbances including the effects of cross-couplings in multivariable systems. By introducing $f(t)$, the process model has changed from second order low pass to a double integrator. Defining an augmented state vector $\boldsymbol{x} = [x_1 \quad x_2 \quad x_3]^T$ with the state variables $x_1 = y$, $x_2 = \dot{y}$ and $x_3 = f$, the process model can be represented as

$$\begin{aligned}\begin{pmatrix}\dot{x}_1\\ \dot{x}_2\\ \dot{x}_3\end{pmatrix} &= \underbrace{\begin{pmatrix}0 & 1 & 0\\ 0 & 0 & 1\\ 0 & 0 & 0\end{pmatrix}}_{\boldsymbol{A}} \cdot \begin{pmatrix}x_1\\ x_2\\ x_3\end{pmatrix} + \underbrace{\begin{pmatrix}0\\ a_0\\ 0\end{pmatrix}}_{\boldsymbol{b}} \cdot u(t) + \begin{pmatrix}0\\ 0\\ 1\end{pmatrix} \cdot \dot{f}(t)\\ y(t) &= \underbrace{\begin{pmatrix}1 & 0 & 0\end{pmatrix}}_{\boldsymbol{c}^T} \cdot \begin{pmatrix}x_1\\ x_2\\ x_3\end{pmatrix}\end{aligned} \tag{3}$$

The basic idea of ADRC is to design an extended state observer (ESO) that provides an estimate of the generalized disturbance $\hat{f}(t)$ - the third state variable in the extended state vector - and to design a control law that compensates its effect on the process. The Luenberger observer equations can be written as

$$\dot{\hat{\boldsymbol{x}}}(t) = \boldsymbol{A}\,\hat{x}(t) + \boldsymbol{b}\,u(t) + \boldsymbol{l}\left(y(t) - \hat{x}_1(t)\right) \tag{4}$$

or

$$\begin{pmatrix}\dot{\hat{x}}_1\\ \dot{\hat{x}}_2\\ \dot{\hat{x}}_3\end{pmatrix} = \begin{pmatrix}-l_1 & 1 & 0\\ -l_2 & 0 & 1\\ -l_3 & 0 & 0\end{pmatrix} \cdot \begin{pmatrix}\hat{x}_1\\ \hat{x}_2\\ \hat{x}_2\end{pmatrix} + \begin{pmatrix}0\\ a_0\\ 0\end{pmatrix} \cdot u(t) + \begin{pmatrix}l_1\\ l_2\\ l_3\end{pmatrix} \cdot y(t) \tag{5}$$

The ESO then estimates $\hat{y} = \hat{x}_1$, $\hat{\dot{y}} = \hat{x}_2$ and $\hat{f} = \hat{x}_3$ from measured process inputs $u(t)$ and outputs $y(t)$.

In the case of a second order process, a linear (modified) PD controller is able to reject the disturbance $f(t)$. The controller equation is

$$u(t) = \frac{u_0(t) - \hat{f}(t)}{a_0} \text{ with } u_0(t) = K_P\left(r(t) - \hat{y}(t)\right) - K_D\hat{\dot{y}}(t) \tag{6}$$

Assuming good estimates and inserting Eq. (6) into Eq. (2) gives

$$\ddot{y}(t) = \left(f(t) - \hat{f}(t)\right) + u_0(t) \approx u_0(t) \approx K_P(r(t) - y(t)) - K_D\dot{y}(t) \tag{7}$$

This finally leads (under ideal conditions) to

$$\frac{1}{K_P}\ddot{y}(t) + \frac{K_D}{K_P}\dot{y}(t) + y(t) = r(t) \tag{8}$$

which guarantees $y(t) = r(t)$ in steady state. The remaining tasks are to tune the controller parameters K_P and K_D, and to specify the observer dynamics by selecting appropriate values for the observer gains $\boldsymbol{l} = (l_1 \quad l_2 \quad l_3)^T$. A practical approach for controller tuning is to specify critically damped closed-loop setpoint tracking dynamics with a user-specified 2% settling time T_{settle}. Then, the controller parameters can be chosen to get a negative real double pole $s_{CL} = -6/T_{settle}$ for equ. (8) which leads to

$$K_P = \left(s_{CL}\right)^2 = 36/T_{settle}^2 \text{ and } K_D = -2 \cdot s_{CL} = 12/T_{settle} \tag{9}$$

If one specifies the ESO dynamics using three poles with a common pole location $s_{ESO} = 3 \cdot s_{CL} \cdots 10 \cdot s_{CL}$ which is fast enough compared with the control loop dynamics, the observer gains can be calculated:

$$l_1 = -3 \cdot s_{ESO}\,,\ l_2 = 3 \cdot \left(s_{ESO}\right)^2 \text{ and } l_3 = -\left(s_{ESO}\right)^3 \tag{10}$$

The resulting control structure is presented in Fig. 1.

In a similar way, ADRC can be designed for a first order process (model), see (Herbst, 2013). In this case, the observer equations are

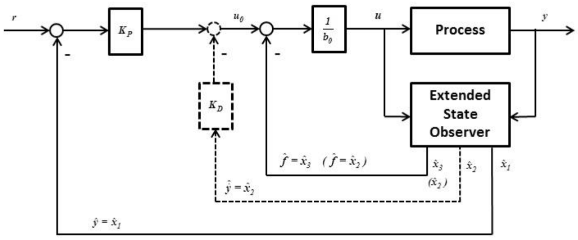

Fig. 1: ADRC control structures for first and second order processes (dashed: extension for second order plan)

$$\begin{pmatrix} \dot{\hat{x}}_1 \\ \dot{\hat{x}}_2 \end{pmatrix} = \begin{pmatrix} -l_1 & 1 \\ -l_2 & 0 \end{pmatrix} \begin{pmatrix} \hat{x}_1 \\ \hat{x}_2 \end{pmatrix} + \begin{pmatrix} a_0 \\ 0 \end{pmatrix} \cdot u(t) + \begin{pmatrix} l_1 \\ l_2 \end{pmatrix} \cdot y(t) \tag{11}$$

and the control law is simplified to a P control law

$$u(t) = \frac{u_0(t) - \hat{f}(t)}{a_0} \text{ with } u_0(t) = K_P\left(r(t) - \hat{y}(t)\right) \tag{12}$$

with $a = K / T$. The controller parameter and observer gains are in this case

$$K_P = -s_{CL} = 4 / T_{settle} \text{ , } l_1 = -2 \cdot s_{ESO} \text{ , } l_2 = \left(s_{ESO}\right)^2 \tag{13}$$

In the first order case, the ADRC control scheme in Fig. 1 does not contain the signal path marked with dashed lines, and only two states ($\hat{x}_1 = \hat{y}$ and $\hat{x}_2 = \hat{f}$) are estimated and fed back to the controller.

In both cases, the only information required to design the ADRC scheme is an estimate of $a_0 \approx K / T^2$ (or $a_0 \approx K / T$, respectively), the desired settling time for the closed loop, and the distance between the observer and the control loop dynamics. For the selection of the observer pole locations, a compromise between estimation speed and noise sensitivity must be found.

3. PROCESS DESCRIPTION

The forced circulation evaporator model first presented by Newell and Lee (1989) has often been used as a benchmark for the application of advanced control technologies. The evaporation process is shown in Fig. 2.

The feed stream which contains at least one non-volatile component is mixed with recirculating liquor and pumped to a vertical heat exchanger. Here, latent heat from condensing steam is used to boil the mixture which is passed to a separation vessel. The vapour is condensed by cooling with water as a coolant. The liquid is recirculated while a part of it is drawn off as the product stream. The variables Fi, Xi and Ti denote the flow rates, compositions and temperatures of stream i , while Li, Pi and Qi are levels, pressures and heat duties in unit i . The model consists of the following differential and algebraic equations:

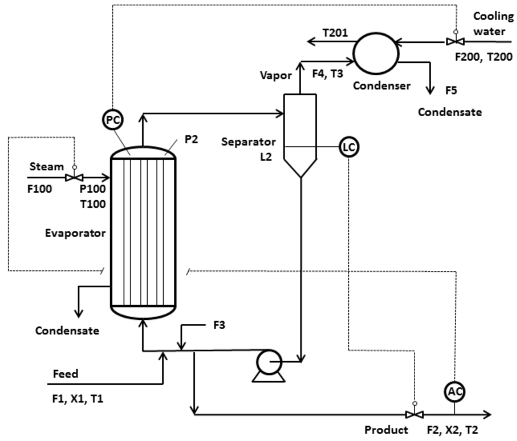

Fig. 2: Evaporator system (Newell and Lee, 1989)

Separator: The mass balance gives

$$\rho A \frac{dL2}{dt} = F1 - F4 - F2 \tag{14}$$

where ρ is the liquid density, and A is the cross-sectional area of the separator.

Evaporator: The mass balances for the liquid solute and the vapour are

$$M \frac{dX2}{dt} = F1 \cdot X1 - F2 \cdot X2 \tag{15}$$

$$C \frac{dP2}{dt} = F4 - F5 \tag{16}$$

where M denotes the constant liquid holdup in the evaporator, and C is a constant that converts the mass of vapour into an equivalent pressure. The liquid and vapour temperatures are calculated from

$$T2 = 0.5616 \cdot P2 + 0.3126 \cdot X2 + 48.43 \tag{17}$$

$$T3 = 0.507 \cdot P2 + 55 \tag{18}$$

These equations result from a linearization of the saturated liquid line for water. The dynamics of the energy balance is assumed to be very fast, therefore

$$F4 = (Q100 - F1 \cdot C_P \cdot (T2 - T1)) / \lambda \tag{19}$$

holds. Here, C_P and λ denote the heat capacity and the latent heat of vaporization of the liquor, respectively.

Steam jacket: For the steam side of the evaporator, fast dynamics is assumed as well. Therefore, the steam jacket is modelled by three algebraic equations:

$$T100 = 0.1538 \cdot P100 + 90 \tag{20}$$

$$Q100 = 0.16 \cdot (F1 + F3) \cdot (T100 - T2) \tag{21}$$

$$F100 = Q100 / \lambda_S \tag{22}$$

with λ_S as latent heat of saturated steam .

Condenser: Again, fast dynamics is assumed leading to the algebraic condenser equations

$$Q200 = \frac{UA2 \cdot (T3 - T200)}{1 + UA2 / (2 \cdot C_P \cdot F200)} \tag{23}$$

$$T201 = T200 + Q200 / (C_P \cdot F200) \tag{24}$$

$$F5 = Q200 / \lambda \tag{25}$$

where $UA2$ denotes the product of the overall heat transfer coefficient of the condenser and the heat transfer area. More details about the modelling assumptions together with the nominal steady-state conditions and the values of the model parameters can be found in (Newell and Lee, 1989).

In the context of control design, the state (and also the output) vector is

$$\boldsymbol{x} = \begin{bmatrix} L2 & P2 & X2 \end{bmatrix}^T \tag{26}$$

The manipulated variables are

$$\boldsymbol{u} = \begin{bmatrix} F2 & F200 & P100 \end{bmatrix}^T \tag{27}$$

and the disturbance variables

$$\boldsymbol{d} = \begin{bmatrix} F1 & T1 & X1 & F3 & T200 \end{bmatrix}^T \tag{28}$$

The separator level is an integrating process and must be controlled. As in (Huusom and Jorgensen, 2014), a PI controller was used for level control with the product flow rate $F2$ as manipulated variable, with a controller gain of $K_C = -1.33$ and a reset time of $T_i = 20\,min$ (SIMC tuning rules). The remaining control variables are the evaporator pressure $P2$ and the product concentration $X2$. In (Newell and Lee, 1989), for single loop PI control the CV/MV-pairings X2 - P100 and P2 - F200 were selected. The resulting single loop control structure is shown in Fig. 1. In practice, P100 and F200 would be controlled by a slave controller, and X2 and P2 by a primary controller in a cascade control structure. Since the dynamics of the secondary control loops is much faster than the open loop dynamics of the primary control variables, subordinate PI controllers were omitted in this study.

The static Relative Gain Array (RGA) can be calculated after the process model is linearized around the steady-state nominal operating point (Newell and Lee, 1989):

$$RGA = \begin{array}{c c} & \begin{array}{cc} P100 & F200 \end{array} \\ \begin{array}{c} X2 \\ P2 \end{array} & \begin{bmatrix} 0.482 & 0.518 \\ 0.518 & 0.482 \end{bmatrix} \end{array} \tag{29}$$

This RGA matrix indicates strong interaction in the multivariable system. Fig. 3 presents the open-loop step responses ($\Delta F200 = +10\,kg/min, \Delta P100 = +10\,kPa$) of the nonlinear evaporator system model when the level controller is in automatic mode.

An attempt to tune PI controllers for the two loops independently using SIMC tuning rules lead to closed-loop instability of the controlled multivariable system. In (Newell and Lee, 1989), the pressure controller was tuned using the Ziegler-Nichols (ZN) reaction curve method ($K_C = -176.5$, $T_i = 9.77\,min$), and the purity controller using the ZN closed-loop tuning method ($K_C = 1{,}64$, $T_i = 12.5\,min$).

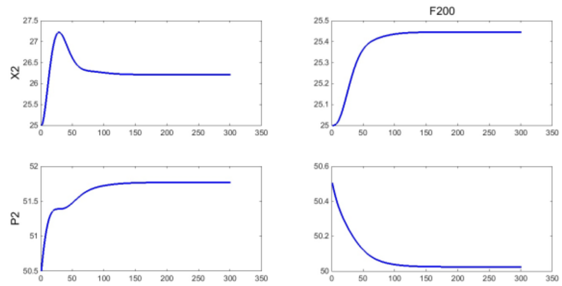

Fig. 3: Evaporator system step responses (first row: X2, second row: P2, left column: P100, right column: F200)

These controller parameters were also used in this paper in order to compare the PI controlled system with ADRC control.

4. IDENTIFICATION OF LOW ORDER MODELS

In practice, a rigorous nonlinear process model is usually not available. Linear ADRC controllers would have to be designed based on low order models identified from active experiments in the plant. To emulate this approach, PRBS test signals were applied to the cooling water flow rate F200 ($\pm 10\,kg/min$) and the steam pressure P100 ($\pm 10\,kPa$), and open-loop simulations of the nonlinear model were carried out to generate "virtual" measurements of the product concentration X2 and the evaporator pressure P2. During the simulations, L2 level control was in automatic mode.

The Matlab System Identification Toolbox was used to identify low order transfer function models. For the MV/CV pair P2 - F200 , the best FOPDT model estimated was

$$G(s) = \frac{-0.051}{33.03s + 1} e^{-0.14s} \tag{30}$$

The estimated dead-time is very short compared to the time constant of the process and will later be neglected in ADRC design. Prediction (one step ahead and pure simulation) of the response based on validation data gives a fit of 95.83%.

Fig. 4 presents the step responses for different linear model approximations of the $X2 - P100$ sub-model. The 4th order state space and ARX models are able to fit the step response of the original nonlinear model, while the FOPDT and SOPDT models have significant errors in both the steady state gain and the transient behaviour.

The best second order process model estimated was

$$G(s) = \frac{0.161}{81.1s^2 + 6.214s + 1} \tag{31}$$

with a model fit of 79.8%. Although this model is certainly not a good approximation of the original "hump" response characteristic (see Fig. 3), it has been deliberately kept for

ADRC design in order to study the effect of un-modelled dynamics.

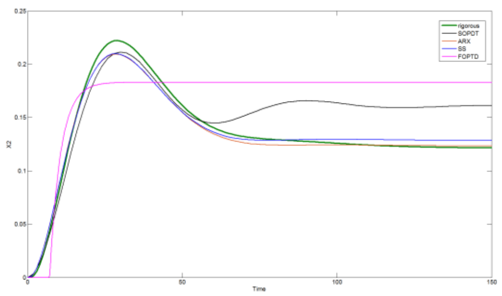

Fig. 4: Step responses of different linear models identified from virtual plant tests.

5. SIMULATION RESULTS

Two SISO ADRC controllers (and related extended state observers) for P2 and X2 have been designed using the procedure explained in section 2. The settling time specifications were 50 minutes for both the pressure and the product purity controllers. This is approximately 50% of the open-loop settling times of the processes. For the P2 ADRC controller, a delay-free model first order model was taken from Eq. (30), while for the X2 ADRC controller the second order process model Eq. (31) was used. The extended state observer dynamics was chosen using $s_{ESO} = 5 \cdot s_{CL}$ for both cases which gave a reasonable compromise between observer dynamics and noise sensitivity. In the sequel, simulation results are presented for the noise-free case only.

Fig. 5 presents the setpoint tracking behaviour of the multi-loop PI and ADRC control systems. For P2, ADRC and PI control give similar settling times, PI control has 10% overshoot but a smaller rise time. The cross-coupling effect on X2 is much smaller for ADRC as for PI control. For X2, the settling time for PI control is twice as much as for ADRC. Regarding the effect on X2, the maximum deviation of X2 is smaller for PI control, while the settling times are similar. ADRC leads to little more aggressive P100 and F200 movements (not shown here). Much shorter settling times are achievable with ADRC without increasing the overshoot, but that would lead to extensive MV movements.

Fig. 6 shows the response to a step change in the feed flow rate and feed composition (external disturbances $\Delta F1 = 0.5 kg / min$, $\Delta X1 = 1\%$).

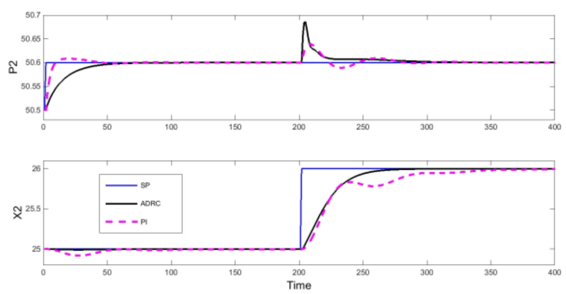

Fig. 5: Closed-loop simulation with setpoint step changes in P2 and X2 (black: ADRC, dashed magenta: PI)

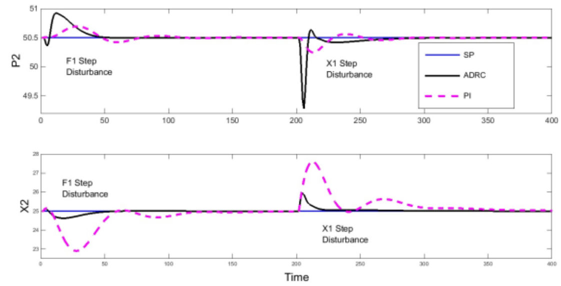

Fig. 6: Closed-loop simulation with step changes in F1 and X1 (black: ADRC, dashed magenta: PI)

ADRC control provides a much better disturbance rejection for the product concentration X2. For P2, ADRC gives shorter settling times (in particular for the feed flow rate disturbance), but a bigger maximum deviation from setpoint. Again, manipulated variable movements are a little more aggressive in case of ADRC control.
Fig. 7 presents the response to a step change in the heat transfer coefficient of the condenser (internal disturbance).

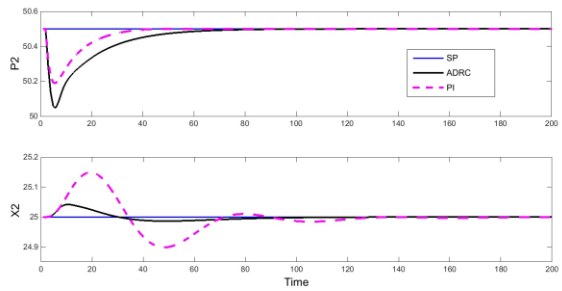

Fig. 7: Closed-loop simulation with step change in UA2 (black: ADRC, dashed magenta: PI)

Again, ADRC provides a much better disturbance rejection for X2. The settling time is halved, and the maximum deviation from setpoint is less than one third compared with PI control. On the other hand, PI gives a better performance for pressure control.
Next, the robustness of the control structures with respect to changes in the process gains has been studied. To do that, the process gains were varied in the range of

$$0,5 \cdot K_{P,nom} \leq K_{P,nom} \leq 1,5 \cdot K_{P,nom} \quad (32)$$

and the setpoint step and disturbance responses have been simulated again. Figs. 8 and 9 show the results for the nominal gains and for the lower and higher limits in gain variation.

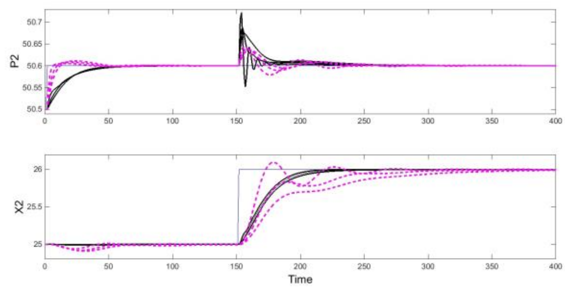

Fig. 8: Robustness of the setpoint tracking performance (black: ADRC, dashed magenta: PI)

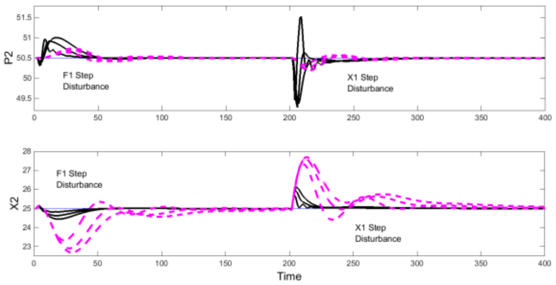

Fig. 9: Robustness of the disturbance rejection performance (black: ADRC, dashed magenta: PI)

For product concentration X2, ADRC is obviously more robust with respect to process gain variation than PI control, in fact for both setpoint tracking and disturbance rejection. For evaporator P2 control, PI control provides more favourable results with respect to smoothness of response and control effort.

6. CONCLUDING REMARKS

Multi-loop linear ADRC control has been applied for the nonlinear Newell-Lee evaporator system benchmark and compared with multi-loop PI control using originally proposed tuning parameters. For product concentration (X2) control, ADRC provides better setpoint tracking as well as disturbance rejection performance. In addition, better robustness properties are achieved for process gain changes. For evaporator pressure (P2) control, performance and robustness of the ADRC and the PI controlled systems are similar, i.e. ADRC does not provide a striking advantage. Interestingly, MPC control based on 4^{th} order ARX models which has been studied in (Huusom and Jorgensen, 2014) gives inferior results for disturbance rejection compared with both PI and ADRC control. This may partly be due to conservative MPC tuning used in this study.

The major advantage of ADRC is the simplicity and transparency of tuning, since only coarse information about the process and the desired closed-loop settling times have to be provided. The performance of ADRC could possibly be improved by applying the nonlinear control algorithm originally proposed by (Han, 2009). On the other hand, better performance of the multi-loop PI control could be achieved when a multi-loop controller tuning approach would be applied (Trierweiler, Müller and Engel, 2001; Dittmar et al., 2012).

In future work, practically important issues such as discrete-time realization of the ESO, consideration of input constraints, sensitivity to measurement noise and its relation to the necessary observer dynamics will be addressed. ADRC modifications for the important class of processes with considerable dead-time have just recently been published (Zhang and Gao, 2014; Zhao and Gao, 2014).

If ADRC will become an alternative to PID and MPC control for industrial control practitioners also depends on the availability of user-friendly off-line design and simulation tools. In addition, Programmable Logic Controllers (PLC) and Distributed Control Systems (DCS) vendors are challenged to pick up ADRC technology and to develop reliable software function block libraries.

REFERENCES

Dittmar, R., Gill, S., Singh, H., Darby, M. (2012). Robust optimization-based PID controller tuning: A new tool and its industrial application. *Contr. Eng. Pract.,* **20,** 355 – 370.

Gao, Z.. (2006). Active Disturbance Rejection Control: A paradigm shift in feedback control system design. *Proc. American Control Conference*, *Minneapolis*, 2399 – 2405.

Han, J. (2009). From PID to Active Disturbance Rejection Control. *IEEE Trans. Ind. Electr.,* **56,** 900 – 906.

Herbst, G. (2013). A simulative study on Active Disturbance Rejection Control as a control tool for practitioners. *Electronics,* **2,** 246 - 279.

Huang, C.E., Li, D, Xue, Y. (2013). Actice Disturbance Rejection Control for the ALSTOM gasifier benchmark problem. *Contr. Eng. Pract.,* **21,** 556 – 564.

Huang, Y., Xue, W. (2014). Active Disturbance Rejection Control: methodology and theoretical analysis. *ISA Trans.,* **53,** 963 – 976.

Huusom, J.K., Jorgensen, J.B. (2014). A realistic process example for MIMO MPC based on autoregressive models. *19th IFAC World Congress, Cape Town, South Africa.*

Lu, J. (2004). An efficient single-loop MPC for replacing PID. *AIChE Annual Conference, Austin, TX.*

Morrison, D. (2005). Is it time to replace PID? *InTech Magazine, March 2005.*

Newell, R.B., Lee, P.L. (1989). *Applied Process Control: A Case Study.* Prentice Hall, New York.

Ogunnaike, B., Mukati, K. (2006). An alternative structure for next generation regulatory controllers. *Journal of Process Control,* **16,** 499 – 509.

Pannocchia, G., Laachi, N., Rawlings, J.B. (2005). A candidate to replace PID control: SISO-constrained LQ control. *AIChE Journal.,* **51,** 1178 – 1189.

Rhinehart, R.R., Darby, M.L, Wade, H.L. (2011). Choosing advanced control. *ISA Trans.,* **50,** 2 – 10.

Richalet, J., O'Donovan, D. (2009). *Predictive Functional Control.* Springer, London.

Trierweiler, J.O., Müller, R., Engell, S. (2001). Multivariable low order structured-controller design by frequency response approximation. *Braz. J. Chem. Eng.,* **17(4-7),** 793 – 807.

Zhao, S., Gao, Z. (2014). Modified active disturbance rejection control for time-delay systems. *ISA Trans.,* **53,** 882 – 888.

Zheng, Q., Chen, Z., Gao, Z. (2009). A practical approach to disturbance decoupling control. *Contr. Eng. Pract.,* **17,** 1016 – 1025.

Zheng, Q., Gao, Z. (2010). On practical applications of Active Disturbance Rejection Control. *Proc. Chinese Control Conference, Beijing,* 6095 – 6100.

Zheng, Q., Gao, Z. (2014). Predictive active disturbance rejection control for processes with time delay. *ISA Trans,* **53,** 873 – 881.